JOURNAL OF MATERIALS SCIENCE **40** (2005) 3917–3920

Void formation and cracking of $Zr_{41}Ti_{14}Cu_{12.5}Ni_{10}Be_{22.5}$ bulk metallic glass under planar shock compression

C. YANG
Key Laboratory of Metastable Materials Science & Technology, Yanshan University, Qinhuangdao 066004, People's Republic of China; Institute of Physics, Chinese Academy of Sciences, Beijing 100080, People's Republic of China
E-mail: chaoyang666@hotmail.com

R. P. LIU*, B. Q. ZHANG, Q. WANG
Key Laboratory of Metastable Materials Science & Technology, Yanshan University, Qinhuangdao 066004, People's Republic of China

Z. J. ZHAN, L. L. SUN, J. ZHANG
Institute of Physics, Chinese Academy of Sciences, Beijing 100080, People's Republic of China

Z. Z. GONG
Institute of Physics, Southwest Jiaotong University, Chengdu, Sichuan 610031, People's Republic of China

W. K. WANG
Key Laboratory of Metastable Materials Science & Technology, Yanshan University, Qinhuangdao 066004, People's Republic of China; Institute of Physics, Chinese Academy of Sciences, Beijing 100080, People's Republic of China

Planar shock compression effects on void formation and cracking in $Zr_{41}Ti_{14}Cu_{12.5}Ni_{10}Be_{22.5}$ bulk metallic glass (BMG) are studied in this paper. Cracking was found to be a result of void linkage in some direction deviation from the maximum shear stress plane. Changing the state of the stress inside the BMG sample led to formation of different void distribution. Nucleation of the microvoids was possibly initiated by release of excess free volume under shock wave compression.

1. Introduction

Multicomponent $Zr_{41}Ti_{14}Cu_{12.5}Ni_{10}Be_{22.5}$ bulk metallic glass (BMG) [1] with extremely high glass forming ability has recently gained considerable attention due to its low density, high strength and fracture toughness, good corrosion and wear resistance, excellent ductility and uniquely dynamical deformation characteristics such as adiabatic shear banding and localized adiabatic heating [2–7]. Lots of work on damage behaviors of $Zr_{41}Ti_{14}Cu_{12.5}Ni_{10}Be_{22.5}$ BMG under uniaxial compression [7–9], tension [10–12] and shocking by light gas gun [13] have been carried out in past studies with particular emphases on low and medium strain rate response of the BMGs. Recently special attention has been given to fracture of BMG as well as nanostructural materials [14–18]. Three fracture criteria were developed for isotropic materials with high strength, such as advanced BMGs or the newly developed bulk nanostructural materials [14].

Unfortunately, little research work has been reported on high-speed impact on BMGs by two-stage light gas gun. The target materials impacted by high-speed projectiles are compressed and then decompressed within extremely short duration. Not only some macroscopic damages (such as fracture cracks) appear after shock loading, but also can some microscopically damaged defects (such as microvoids) formed during shock loading possibly be persevered inside target body, which have the same formation characteristics as excess free volume frozen inside the BMG during rapid quenching solidification [19]. Formation of fracture cracks are always related to appearance of these damaged defects nucleated from intrinsic defects of BMG. Therefore, cracking or fracture at an extremely high strain rate may give some clues to reveal the structure-related features of BMGs. In this paper, crack formation and propagation inside the $Zr_{41}Ti_{14}Cu_{12.5}Ni_{10}Be_{22.5}$ BMG under compressive shock wave at velocities of 2.7 and

*Author to whom all correspondence should be addressed.

3.2 km/s with aluminum projectiles launched by a two-stage light gas gun were presented.

2. Experimental procedure

Ingots of the alloy with a nominal composition of $Zr_{41}Ti_{14}Cu_{12.5}Ni_{10}Be_{22.5}$ were prepared from mixture of pure elements in an arc-melting furnace under Ti-gettered argon atmosphere. The purity of Zr, Ti, Cu, Ni and Be were 99.999, 99.9, 99.5, 99 and 99.5% respectively. The ingots were then melted again in quartz tubes, and quenched into water to obtain BMG rods 18 and 22 mm in diameter. Small cylindrical samples cut from the alloy rod were used as targets for high-speed impact experiments. Structures of the BMG samples before high-speed impact experiments were identified to be full amorphous state by a D/max-2500/pc X-ray diffraction patterns (XRD) (Cu K_α). During the impact experiments, the BMG target samples were assembled in a recovery device, as shown in Fig. 1. The assembly was then inserted into a steel cylinder, the inner and outer diameters of which are 40 and 120 mm respectively. The target sample, 17.5 mm in diameter and 10 mm in thickness, was impacted by a planar shock wave with an aluminum flyer, 24 mm in diameter and 2 mm in thickness, launched at the speed of 2.7 km/s by a two-stage light gas gun [20]. The use of the cylindrical flyer with a larger size in diameter than that of the sample was to guarantee to produce a planar shock wave on the top surface of the sample. Another impact experiment was carried out using the same recovery device, but the BMG sample was directly exposed to the spherical projectile fired at a speed of 3.2 km/s instead of covering by a thin copper plate in the planar shock wave test. In addition, the BMG target was 22 mm in diameter and 10 mm in thickness, and the projectile was 5 mm in diameter in this case. The impacted samples were afterwards cut out from the assembly with an electric spark-cutting machine, and sectioned, ground and polished for microstructure examination with a XRD and an XL30 S-FEG type high-resolution scanning electron microscopy (SEM).

3. Results and discussion

After the planar shock wave impact at the speed of 2.7 km/s, the sample size was changed from 17.5 into 20.5 mm in diameter and from 10.0 into 7.3 mm in thickness under the effect of strong compressive wave (in this case, peak pressure in the sample reached about 34 GPa). The front surface of the sample that faced the flyer exhibited dense cracks. Cracking was reasonable because the compressive stress used in the present case was far above the strength limit of the BMG. Fig. 2 shows SEM micrographs of the cross-section of the BMG target. A crack in the front surface layer, as seen in Fig. 2a, is found in the compressed sample. The angle θ between the shock direction and the fracture plane was around 35° if compensation of the size change caused by the compression is considered. The present result on θ is significantly deviated from the Tresca criterion [21] but in agreement with the recent result on deviation of θ angle by Zhang *et al.* [14–15]. In the central part of the compressed sample along the compressive direction, cracking exhibits a different feature. Intersection of cracks can be found, as shown in Fig. 2b. Two cracks perpendicular to each other propagated and ended at a point where they met, forming a "T"-shaped crack pattern. The intersection of cracks as well as the θ angle deviation from the theoretical 45° was probably caused by a complex stress state inside the sample led by the interplay of the vertical loading shock wave and the reflected waves from the restrained walls of the sample container. The interplay of the shock waves led to the deviation of the highest shear stress plane from the theoretical direction of 45° relative to the loading direction. At a bottom position inside the sample, a more complex stress state was formed and a larger deviation of the θ angle from 45° was found. Detailed observation of the crack marked by the rectangle area in Fig. 2b shows that the cracks were in fact just a result of coalescence of some small voids formed in some shear stress direction, as shown in Fig. 3. Traces of the spherical voids as well as their linkage to form cracks can clearly be found. From these observations, one may extrapolate that the crack in Fig. 2a was also formed by coalescence of voids, but the void are too small to be distinguished from the crack in the firstly impacted upper layer of the sample. It seems that the voids were formed along some shear stress plane and influenced by the stress distribution inside the sample.

In order to reveal the formation characteristics of the voids as well as their relation to crack propagation during compression, another kind of shock loading experiment was carried out. A spherical projectile of 5 mm in diameter was shoot at a speed of 3.2 km/s to impact a medium thick BMG target of 22 mm in diameter and 10 mm in thickness. In this case, the loading spherical shock waves, causing a peak pressure of about 40 GPa, interacted inside the sample with the reflected waves from the side and the rear surfaces of the sample, and an even more complex stress state than that caused by the planar shock wave was formed as a result. No particular direction was preferable for stress concentration, which, on the other hand, was quite normal in unidirectional compression as loaded by the planar shock wave. This kind of experiment was expected to form different distribution of voids inside the BMG sample from that formed under the planar shock waves. Fig. 4 shows the

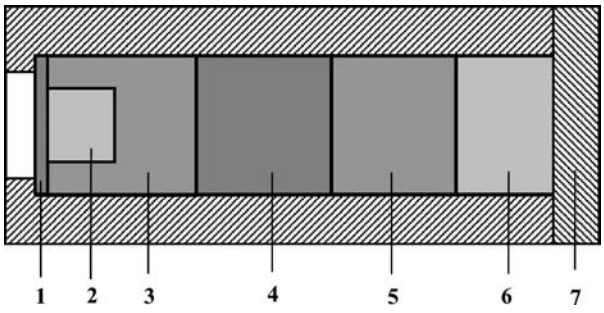

Figure 1 Schematic diagram of the recovery device for hypervelocity impact (1. Copper plate; 2. $Zr_{41}Ti_{14}Cu_{12.5}Ni_{10}Be_{22.5}$ BMG target; 3. Copper cylinder; 4. Aluminum cylinder; 5. Steel cylinder; 6. Polyethylene cylinder; 7. Steel cylinder tube.).

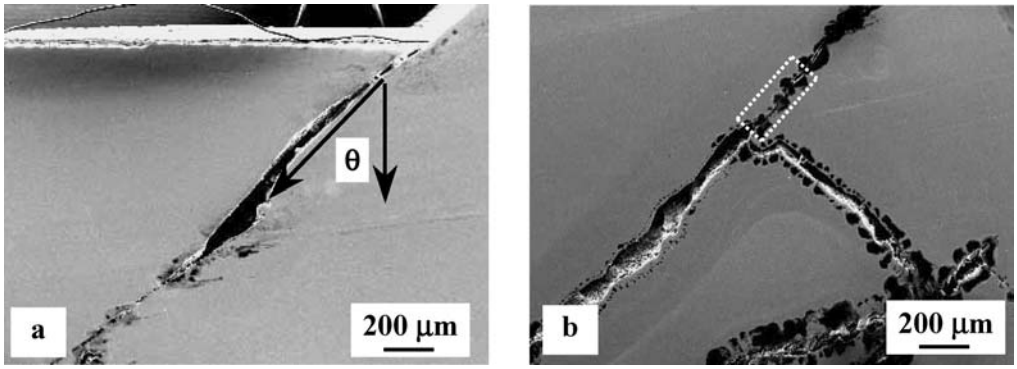

Figure 2 SEM micrographs showing cross-section microstructures of the recovered $Zr_{41}Ti_{14}Cu_{12.5}Ni_{10}Be_{22.5}$ BMG sample under planar shock loading of aluminum flyer with a speed of 2.7 km/s.

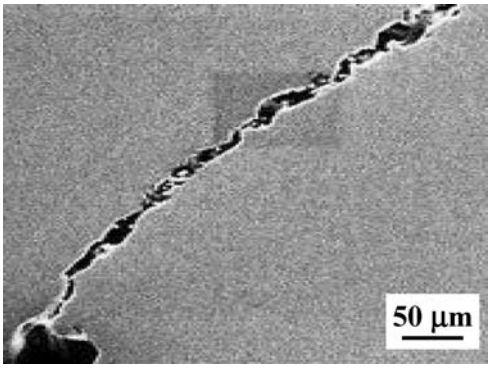

Figure 3 SEM micrographs showing voids coalescence process inside a crack on the cross section of the recovered $Zr_{41}Ti_{14}Cu_{12.5}Ni_{10}Be_{22.5}$ BMG sample under planar shock loading of aluminum flyer with a speed of 2.7 km/s.

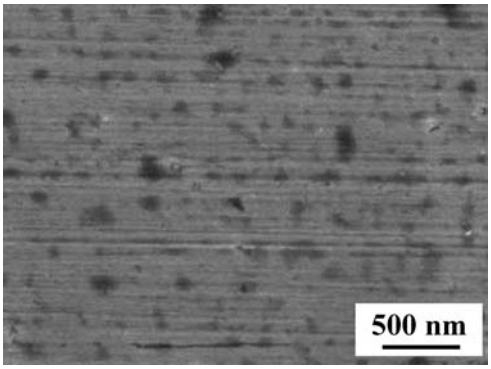

Figure 4 SEM micrograph of morphology showing "frozen in" microvoids on the recovered $Zr_{41}Ti_{14}Cu_{12.5}Ni_{10}Be_{22.5}$ BMG sample under aluminum projectile impact with a speed of 3.2 km/s.

result of the voids formed in the sample impacted by a spherical projectile at the speed of 3.2 km/s. Regions with homogeneously distributed voids can be found as expected for a complex state of stress distribution in the sample. Unlike the planar shock wave that caused the highest shear stress in the direction of 45° (with some deviation in the present experiment) to the loading direction, the complex stress distribution caused the formation of the voids more homogeneous, as seen in Fig. 4. The average size of the voids is around 20 nm, which is comparable to other previous results [3–4].

Voids were suggested to form by nucleation, growth, and coalescence during compression or tension of crystal materials [22]. Multiple impurities and defects such as grain boundaries, inclusions, vacancies, dislocations, twins, and so on are responsible for the microvoid initiation in polycrystalline materials [22–24]. In the metallic glass, free volume is more common than the other defects in crystals. The impurity effect on nucleation of microvoids can be ignored in the BMG sample too. In order to form bulk metallic glass during solidification, the impurity-caused heterogeneous nucleation had to be avoided. If the voids in Fig. 4 were caused by impurities, such a high amount of impurities inside the bulk glass sample were implausible. Such a high amount of impurities homogeneously distributed in the matrix is not a common feature in BMG. Crystallization phenomenon didn't take place in present experiments by the XRD results of recovered samples. Consequently, the formation of the microvoids was most likely related to intrinsic defect of BMG, the excess free volume frozen inside the BMG samples during rapid quenching. In fact, the free volume theory was considered to be appropriate for understanding deformation in metallic glasses [7, 25–27]. As about 1% of excess free volume was frozen inside the BMG during water-quenching solidification [19], release of the excess free volume under shock wave compression possibly initiated the nucleation of microvoids.

It is well accepted that voids can be formed under tension conditions. However, unlike hydrostatic compression, stress state in our cases is characteristics of one dimension strain and three dimensions stress, in which shock compressive stress was much larger than compressive stresses caused by Cu container. When shock wave transmits in isotropic homogeneous BMG, shear stress occurs and possesses maximum value at an angle θ 45° relative to the shock direction, accompanying with the appearance of shock compressive stress. The shear stress increases with the increase of compressive stress. After the shear stress exceeds the shear yield limit of BMG, it keeps unchanged regardless of increase of compressive stress. Thus, plastic flow will occur in the direction of shear stress plane, which is also called adiabatic heat shear band. Because of particular structures of BMG, the shear stress plane deviated from the maximum stress plane in our cases. The heat caused by plastic flow will soften the material, which in turn accelerates the plastic flow. Due to poor thermal conductivity and extremely high strain

rate of BMG, the generated heat far exceeds the dissipated heat. This causes the melt of localized material in adiabatic shear band. Heat softness of BMG will cause the concentration and relaxation of stress, which leads to formation of tension stress. Under tension stress, voids form as a result of release of excess free volume in shear band. Then, voids will coalesce and link to a fracture crack (shear cracks) under high compressive stress.

With the statistical approach [28] used in polycrystalline materials, the voids in Fig. 4 can be estimated with a volume fraction of 2.5%. This amount is comparable to the excess free volume frozen in the BMG. Although it is hard to realize that the excess free volumes inside BMG samples gathered under shock compression, it is not unreasonable to come to the conclusion that these homogeneously distributed voids implies that nucleation of microvoids is most likely related to the release of the excess free volumes under shock compression. It should be noted that the voids volume in Fig. 4 included probably the growth volume of nucleated microvoids under effect of compression and release of stress. Further research work about this aspect will be done in the future.

4. Conclusion

When the BMG target was impacted by a planar shock wave at the speed of 2.7 km/s with an aluminum projectile launched by a two-stage light gas gun, fracture cracks were observed to be a process collapse and linkage of voids in some direction deviating from maximum shear stress plane. Nucleation, growth and linkage of voids in this direction, most probably as a result of free volume release, are considered to be the main reason for fracture of the BMG. When the BMG target was impacted by a spherical projectile, a more complex stress state with no preferable directions was formed by interplay of the spherical shock wave and the reflected waves from the container walls. In this case, homogeneously distributed voids, not as that concentrated along some preferable directions in the planar shock wave impacted sample, were found, which implies that nucleation of microvoids were directly related to the stress state inside the sample.

Acknowledgements

The authors acknowledge financial supports from NSFC (Grant No. 50325103/50271062/50171077).

References

1. X. P. TANG, U. GEYER, R. BUSCH, W. L. JOHNSON and Y. WU, *Nature* **402** (1999) 160.
2. F. SPAEPEN, *Acta Metall.* **25** (1977) 407.
3. A. S. ARGON, *ibid.* **27** (1979) 47.
4. P. S. STEIF, F. SPAEPEN and J. W. HUTCHINSON, *ibid.* **30** (1982) 447.
5. H. J. LEAMY, H. S. CHEN and T. T. WANG, *Metall. Trans.* **3** (1972) 699.
6. C. T. LIU *et al.*, *Metall. Mater. Trans. A* **29A** (1998) 1811.
7. W. J. WRIGHT, R. B. SCHWARZ and W. D. NIX, *Mater. Sci. Eng. A* **319–321** (2001) 229.
8. G. SUBHASH, R. J. DOWDING and L. J. KECSKES, *ibid.* **334** (2002) 33.
9. C. J. GILBERT, J. W. AGER III, V. SCHROEDER and R. O. RITCHIE, *Appl. Phys. Lett.* **74** (1999) 3809.
10. J. X. LI, G. B. SHAN, K. W. GAO, L. J. QIAO and W. Y. CHU, *Mater. Sci. Eng. A* **00** (2003) 1.
11. K. M. FLORES and R. H. DAUSKARDT, *ibid.* **319–321** (2001) 511.
12. C. J. GILBERT, R. O. RITCHIE and W. L. JOHNSON, *Appl. Phys. Lett.* **71** (1997) 476.
13. S. J. TURNEAURE, J. M. WINEY and Y. M. GUPTA, *ibid.* **84** (2004) 1692.
14. Z. F. ZHANG, G. HE, J. ECKERT and L. SCHULTZ, *Phys. Rev. Lett.* **91** (2003) 045505.
15. Z. F. ZHANG, J. ECKERT and L. SCHULTZ, *Acta Materialia* **51** (2003) 1167.
16. C. A. SCHUH and A. C. LUND, *Nature Mater.* **2** (2003) 449.
17. G. HE, J. ECKERT, W. LOESER and L. SCHULTZ, *ibid.* **2** (2003) 33.
18. E. MA, *Nature Mater.* **2** (2003) 7.
19. C. NAGEL, K. RAETZKE, E. SCHMIDTKE and J. WOLFF, *Phys. Rev. B.* **57** (1998) 10224.
20. A. C. MITCHELL and W. J. MELLIS, *Rev. Sci. Instrum.* **52** (1981) 347.
21. P. E. DONOVAN, *Acta Metall.* **37** (1989) 445.
22. D. R. CURRAN, L. SEAMAN and D. A. SHOCKEY, in "Shock Waves and High-Strain-Rate Phenomena in Metals," edited by M. A. Meyers and L. E. Murr (Plenum Press, New York, 1981) p. 129, 136.
23. A. K. ZUREK, W. R. THISELL, J. N. JOHNSON, D. L. TONKS and R. HIXSON, *J. Mater. Process. Techn.* **60** (1996) 261.
24. D. L. TONKS, *J. Physique IV C8* **4** (1994) 665.
25. W. J. WRIGHT, R. SAHA and W. D. NIX, *Mater. Trans., JIM* **42** (2001) 642.
26. K. M. FLORES, D. SUH, R. HOWELL, P. A. KUMAR, P. A. STERNE and R. H. DAUSKARDT, *Mater. Trans. JIM* **42** (2001) 619.
27. K. M. FLORES and R. H. DAUSKARDT, *Acta Mater.* **49** (2001) 2527.
28. L. SEAMAN, D. R. CURRAN and D. A. SHOCKEY, *J. Appl. Phys.* **47** (1976) 4814.

Received 17 November 2004
and accepted 28 February 2005